

Atomic dynamics in single and multi-photon double ionization: An experimental comparison

Th. Weber, M. Weckenbrock, A. Staudte, M. Hattass, L.
Spielberger, O. Jagutzki, V. Mergel, H. Schmidt Böcking,

Institut für Kernphysik, August Euler Str 6 60486 Frankfurt, Germany

G. Urbasch, H. Giessen

*Fachbereich Physik, Philipps-Universität, Renthof 5, D-35032
Marburg Germany*

H. Bräuning

Strahlencentrum, Leihgesterner Weg 217 D-35392 Giessen, Germany

C.L. Cocke

*Department of Physics, Kansas State University, Manhattan, KS
66506*

M.H. Prior

Lawrence Berkeley National Laboratory, Berkeley, CA 94720

R. Dörner

*Fakultät für Physik, University Freiburg,
Hermann Herder Str. 3, D79104 Freiburg
rdoerner@uni-freiburg.de*

Abstract: We have used a multi-particle imaging technique (COLTRIMS) to observe the double ionization of rare gas atoms by multi-photon absorption of 800 nm (1.5 eV) femto-second laser pulses and by single photon absorption (synchrotron radiation). Both processes are mediated by electron correlation. We discuss similarities and differences in the three-body final state momentum distributions.

© 2001 Optical Society of America

OCIS codes: (020) Atomic and molecular physics (020.4180) Multiphoton Processes

References and links

1. J. Briggs and V. Schmidt, "Differential cross sections for photo-double-ionization of the helium atom," *J. Phys.* **33**, R1 (2000).
2. R. Dörner, V. Mergel, O. Jagutzki, L. Spielberger, J. Ullrich, R. Moshhammer, and H. Schmidt-Böcking, "Cold Target Recoil Ion Momentum Spectroscopy: A 'momentum microscope' to view atomic collision dynamics," *Physics Reports* 330, 96–192 (2000).
3. H.P Bräuning, R. Dörner, C.L. Cocke, M.H. Prior, B. Krässig, A. Bräuning-Demian, K. Carnes, S. Dreuil, V. Mergel, P. Richard, J. Ullrich, and H. Schmidt-Böcking, "Recoil ion and electronic angular asymmetry parameters for photo double ionization of helium at 99 eV," *J. Phys.* **B30**, L649 (1997).
4. H.P Bräuning, R. Dörner, C.L. Cocke, M.H. Prior, B. Krässig, A. Kheifets, I. Bray, A. Bräuning-Demian, K. Carnes, S. Dreuil, V. Mergel, P. Richard, J. Ullrich, and H. Schmidt-Böcking, "Ab-

- solute triple differential cross sections for photo-double ionization of helium - experiment and theory," *J. Phys.* **B31**, 5149 (1998).
5. R. Dörner, J. Feagin, C.L. Cocke, H. Bräuning, O. Jagutzki, M. Jung, E.P. Kanter, H. Khemliche, S. Kravis, V. Mergel, M.H. Prior, H. Schmidt-Böcking, L. Spielberger, J. Ullrich, M. Unverzagt, and T. Vogt, "Fully Differential Cross Sections for Double Photoionization of He Measured by Recoil Ion Momentum Spectroscopy," *Phys. Rev. Lett.* **77**, 1024 (1996).
 6. R. Dörner, H. Bräuning, J.M. Feagin, V. Mergel, O. Jagutzki, L. Spielberger, T. Vogt, H. Khemliche, M.H. Prior, J. Ullrich, C.L. Cocke, and H. Schmidt-Böcking, "Photo-double-ionization of He: Fully differential and absolute electronic and ionic momentum distributions," *Phys. Rev.* **A57**, 1074 (1998).
 7. R. Wehlitz, F. Heiser, O. Hemmers, B. Langer, A. Menzel, and U. Becker, "Electron-energy and -angular distributions in the double photoionization of helium," *Phys. Rev. Lett.* **67**, 3764 (1991).
 8. A. Becker and F.H.M. Faisal, "Interpretation of Momentum Distribution of Recoil Ions from Laser Induced Nonsequential Double Ionization," *Phys. Rev. Lett.* **84**, 3546 (2000).
 9. Th. Weber, M. Weckenbrock, A. Staudte, L. Spielberger, O. Jagutzki, V. Mergel, G. Urbasch, M. Vollmer, H. Giessen, and R. Dörner, "Recoil-Ion Momentum Distributions for Single and Double Ionization of Helium in Strong Laser Fields," *Phys. Rev. Lett.* **84**, 443 (2000).
 10. R. Moshhammer, B. Feuerstein, W. Schmitt, A. Dorn, C.T. Schöter, J. Ullrich, H. Rottke, C. Trump, M. Wittmann, G. Korn, K. Hoffmann, and W. Sandner, "Momentum Distributions of N^{n+} Ions Created by an Intense Ultrashort Laser Pulse," *Phys. Rev. Lett.* **84**, 447 (2000).
 11. R. Moshhammer B. Feuerstein and J. Ullrich, "Nonsequential multiple ionization in intense laser pulses: interpretation of ion momentum distributions within the classical 'rescattering' model," *J. Phys* **B33**, L823 (1992).
 12. K. Sacha and B. Eckhardt, "Pathways to double ionization of atoms in strong fields," *Phys. Rev. A*:accepted for publication 2001, (2001).
 13. L.B. Fu J. Chen, J. Liu and W. M. Zheng, "Interpretation of momentum distribution of recoil ions from laser-induced nonsequential double ionization by semiclassical rescattering model," *Phys. Rev.* **A63**, 011404R (2000).
 14. M. Lein, E.K.U. Gross, and V. Engel "Intense-Field Double Ionization of Helium: Identifying the Mechanism," *Phys. Rev. Lett.* **85**, 4707 (2000).
 15. R. Kopold, W. Becker, H. Rottke, and W. Sandner, "Routes to Nonsequential Double Ionization," *Phys. Rev. Lett.* **85**, 3781 (2000).
 16. Th. Weber, H. Giessen, M. Weckenbrock, A. Staudte, L. Spielberger, O. Jagutzki, V. Mergel, G. Urbasch, M. Vollmer, , and R. Dörner, "Correlated electron emission in multiphoton double ionization," *Nature* **404**, 608 (2000).
 17. K.T. Taylor, J.S. Parker, D. Dundas, E. Smyth and S. Vitirito, "Laser Driven Helium in Full-Dimensionality," *Laser Physics* **9**, 98-116 (1999)
 18. M. Lein, E.K.U. Gross, and V. Engel, "On the mechnism of strong-field double photoionisation in the helium atom," *J. Phys B* **33**, 433-442 (2000)
 19. F. Maulbetsch and J.S. Briggs, "Selection rules for transitions to two-electron continuum states," *J. Phys.* **B28**, 551 (1995).
 20. I.E. McCarthy and E. Weigold, "Electron momentum spectroscopy of atoms and molecules," *Rep. Prog. Phys.* **54**, 789 (1991).
 21. A. Becker and F.H.M. Faisal, "Correlated Keldysh-Faisal-Reiss theory of above-threshold double ionization of He in intense laser fields," *Phys. Rev.* **A50**, 3256 (1994).
 22. J.H. McGuire, N. Berrah, R.J. Bartlett, J.A.R. Samson, J.A. Tanis, C.L. Cocke, and A.S. Schlachter, "The ratio of cross sections for double to single ionization of helium by high energy photons and charged particles," *J. Phys.* **B28**, 913 (1995).
 23. S. Keller, "Perturbation theory for $(\gamma, 2e)$ on helium," *J. Phys.* **B33**, L513 (2000).
 24. Ken-ichi Hino, T. Ishihara, F. Shimizu, N. Toshima, and J.H. McGuire, "Double photoionization of helium using many-body perturbation theory," *Phys. Rev.* **A48**, 1271 (1993).
 25. S. Bhattacharyya and S. Mitra, "Double photoionization of He by circularly polarized light: A QED approach," *Phys. Rev.* **62**, 032709 (2000).
 26. A. Becker and F. H. M. Faisal, "Mechanism of laser-induced double ionization of helium," *J. Phys.* **B29**, L197 (1996).
 27. A. Becker and F.H.M. Faisal, "Interplay of electron correlation and intense field dynamics in the double ionization of helium," *Phys. Rev.* **A59**, R1742 (1999).
-

1 Introduction

Double ionization of atoms by photons has attracted much attention for more than 30 years. This is mainly because it is a direct observation window for many-particle correlation effects. These are a major theoretical challenge for quantum mechanics and have

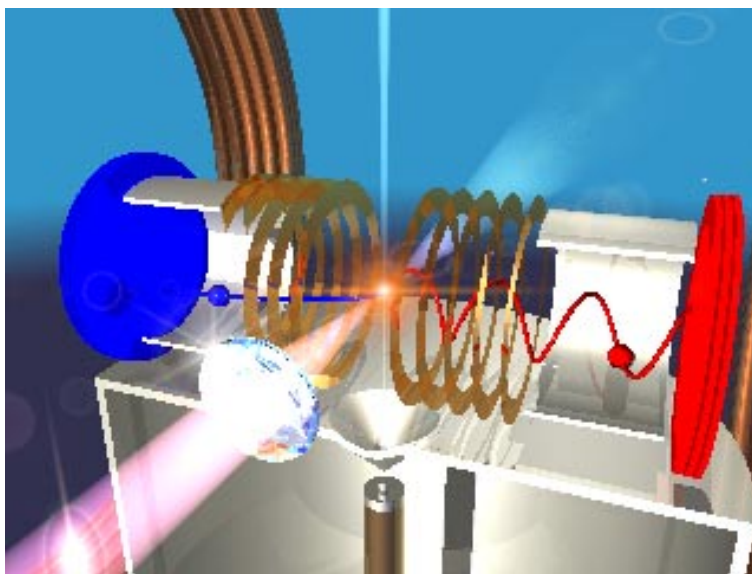


Fig. 1. Experimental setup. Electrons (red) and ions (blue) are created in the supersonic gas jet target. The thin copper rings create a homogeneous electric field, the large Helmholtz coils an additional magnetic field. These fields guide the charged particles onto fast time and position sensitive channel plate detectors (Roentdek www.roentdek.com). Time-of-flight and position of impact of each electron-ion pair is recorded in list mode. From this the three dimensional momentum vector of each particle can be calculated.

far-reaching practical importance in many fields of physics and chemistry. Historically photo double ionization was first studied by absorption of a single photon (see [1] for a recent review); after the advent of powerful femto-second laser pulses the study of the multi-photon regime followed during the last 10-15 years (see the contributions in this issue). In the multi- as well as in the single-photon case, the most detailed experimental observable is the multi-dimensional correlated momentum distribution of the two emitted electrons and the recoiling ion. In the present work we examine this final state momentum space for both processes.

For the single photon case, electron-electron correlation is the only pathway to the double ionization continuum. For the multi-photon case, additionally an ejection of two electrons by two sequential interactions with the laser field becomes possible. In the intensity region of the knee in the double ionization yield it is, however well established now that this sequential process is negligible and it is also electron-electron correlation which mediates the double electron ejection. The details of the correlation mechanism in the single- and multi-photon case will be discussed below guided by experimental observations.

2 Experiment

We have used Cold Target Recoil Ion Momentum Spectroscopy (COLTRIMS) (see [2] for a recent review) to measure in coincidence the momentum vector of one of the electrons and the recoiling doubly charged ion. The experimental setup is shown in figure 1. The atoms are prepared with a very small initial state momentum spread in a supersonic gas jet. The photons are focused into this gas beam. Ions (blue) and electrons (red) are guided by electric and magnetic fields towards two position- and time- sensitive channel-plate detectors facing each other. From the position of impact and the time of

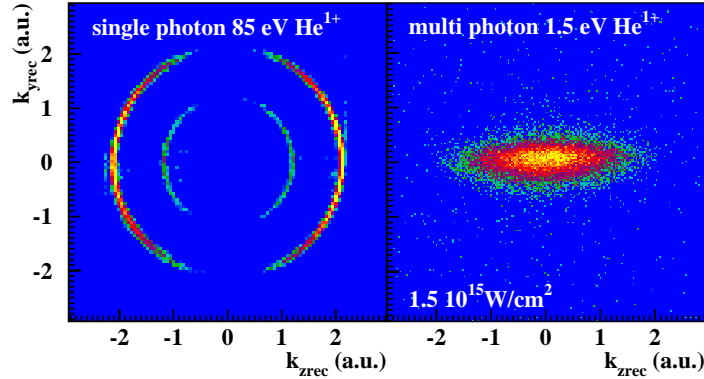


Fig. 2. Momentum distribution of He^{1+} ions. Left: For 85 eV single photon absorption. Right: 1.5 eV (800nm), 220 fsec, $1.4 \times 10^{15} \text{ W/cm}^2$. The polarization vector of the light is horizontal. The photon momentum is vertical. In the left figure the momentum component in the third dimension out of the plane of the figure is restricted to $\pm 0.4 \text{ a.u.}$, the right panel is integrated over the momenta in the direction out of the plane of the figure

flight the starting momentum of the particle is inferred. The time-of-flight is measured with respect to the light pulse. The repetition rate is 3 MHz for the synchrotron and 1 kHz for the femto-second laser. In both cases the gas density is adjusted such that much less than one atom is ionized per pulse in order to avoid false coincidences. For each event we record the position and timing information from both detectors in list mode. Therefore the experiment can be replayed offline and the data can be sorted again as new physical questions arise. The experiments on single photon absorption presented below were performed four years ago (see [3, 4, 5, 6] for discussion of other aspects of these experiments) they have been resorted in the present context to allow for direct comparison with the data for multi-photon ionization.

3 Single Ionization

The momentum distribution of He^+ ions created by 85 eV linear polarized photons and by 1.5 eV (800 nm), 220 fsec, $1.4 \times 10^{15} \text{ W/cm}^2$ laser light are shown in figure 2. In both cases the photon momentum is negligible on the scale of the figure (an 85eV photon has 0.02 a.u. momentum). Therefore, due to momentum conservation, the ion and electron are emitted with almost equal and opposite momentum. The ion momentum distribution is just a mirror image of the electron distribution. The outer ring in figure 1a corresponds to ions in the ground state, the inner rings to the excited states of the He^+ ion. For the single photon case the electron energy is determined by the photon energy, leading to discrete rings. In the multi-photon case no ATI structure (isolated peaks in the energy distribution) is observed. In the present experiment this might be due to our resolution, however even for high resolution electron spectroscopy no ATI structure is found for He at this intensity. A very different angular distribution is observed in the two cases. For the single-photon case the ground state (main) line shows a dipole distribution. In the multi-photon case, however, at least 17 photons must be absorbed to overcome the binding energy. Therefore high angular momentum states can in principle be populated allowing for a highly directed breakup of the atom along the polarization vector. In a simple two step picture one can assume the electron to tunnel through the barrier of the joint optical and atomic potential. Once set free the

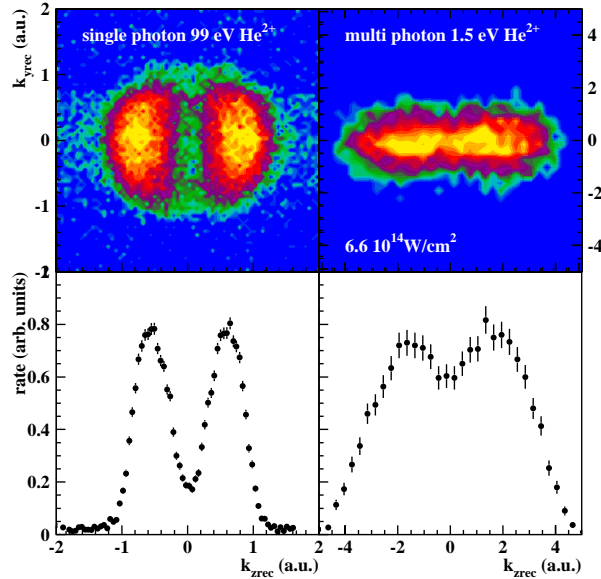


Fig. 3. Momentum distribution of He^{2+} ions. Left: For 99 eV single photon absorption. Right: 1.5 eV (800nm), 220 fsec, $6.6 \times 10^{14} \text{ W/cm}^2$. The polarization vector is horizontal. The two bottom panels show projections of the distributions on the polarization axis.

electron and the ion are accelerated by the laser field. The net momentum transferred from the field depends only on the phase at the instant of ionization with momentum zero corresponding to the field maximum.

4 Double Ionization

The ratio of double to single ionization for Helium is about 2 % for 100 eV single-photon absorption and is only about 0.09 % for 1.5 eV photons at 220 fsec $6.6 \times 10^{14} \text{ W/cm}^2$. The momentum distributions of the doubly charged ions parallel to the polarization, however, show surprising similarities (figure 3). In both cases a double peak structure with a minimum at momentum zero is found. For single-photon absorption this minimum holds for all photon energies investigated so far [3, 5, 6]. In both cases the double peak structure can be understood as a consequence of an electron-electron scattering being responsible for the ejection of the second electron. The scenarios for this electron scattering however are very different.

For the single photon case in a first step the dipole operator acts on the charge dipole in the atom, which consist of the nucleus on one end and one electron (or the center of charge of the two electrons) on the other end. The absorption of the photon imprints its dipolar characteristics onto the breakup of this charge dipole. On the way out of the atom the electron scatters inelastically at the second electron leading to double electron ejection. This electron-electron interaction smears out the orientation of the initial absorption in the electron distribution. The electrons are emitted almost isotropic [3, 7]. The recoil nucleus however keeps a memory of the absorption step (figure 3a); its momentum distribution is a reminiscence of the single ionization case (figure 2a). The two peaks result from this dipolar emission characteristic.

In the multi-photon case (figure 3b) the peaks result from the acceleration of the doubly charged ion in the laser field. This has been demonstrated strikingly by A. Becker

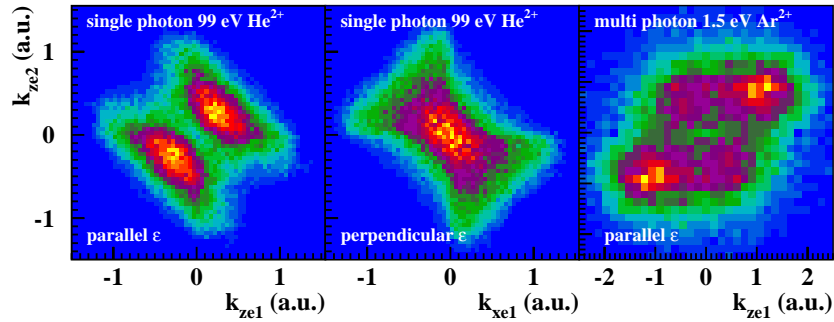


Fig. 4. Momentum correlation between the two emitted electrons. Left and middle: Helium, doubly ionized by absorption of one 99eV photon. Left: The horizontal axis shows the momentum components of one electron along the polarization axis, the vertical axis the same momentum component of the corresponding second electron. Middle: Like left, but the momentum components along an axis perpendicular to the polarization is shown. The Quicktime movie (0.7MB) shows the transition between the left and middle distribution. I.e. the axis along which the momentum components are taken is rotating as indicated by the red double arrow. Right: Corresponding figure to the left one but for multi-photon double ionization of Argon by in the focus of a 220 fsec, 800nm laser pulse at peak intensities of $3.8 \cdot 10^{14}$ W/cm². In all three figures the same sign of the momenta for both electrons means emission to the same half sphere, however the plane which divides the two half spheres is rotated in the middle panel. The data are integrated over the momentum components in the direction perpendicular to the polarization. The color coding shows the differential rate on linear scale in arbitrary units.

and Faisal [8]. They have shown that the double peak structure vanishes if one neglects the interaction with the laser field after ionization of the second electron. The peak position is in agreement with the most simple classical rescattering model and can be predicted by calculating the phase at the instant of recollision (see [9, 10, 11]). This conclusion has been confirmed using Wannier type arguments [12], a more elaborate semi-classical rescattering model [13], one dimensional calculation [14] and S-Matrix calculations [15]. Here the double ionization ion momentum is very different from the single ionization case, which peaks at zero momentum. Thus the similarity between the momentum distribution of the ions in the single and multi-photon case is fortuitous. The physical scenario leading to the two peaks is very different in the two cases.

More detailed information about the double ionization process can be obtained from the momentum correlation of the emitted electrons. We have reported previously that for the multi-photon case, the electrons are emitted preferentially in the same direction with a similar momentum [16]. In figure 4 we compare these results with similar presentation for single photon absorption. For the strong field case, again, the rescattering model provides a qualitative explanation for the observations. For double ionization to happen the primary electron has to have on its return sufficient energy to at least excite the parent ion. For Ar⁺ the first excited states are around 16-17 eV. In order to have this return energy at the $3.8 \cdot 10^{14}$ W/cm² the primary electron has to return at a phase of about 35 deg off the field maximum. The electron will then be stopped by the excitation, the second electron will be field ionized and hence both electrons start with almost zero momentum in the laser field. Finally the starting phase of 35 deg will lead to a drift momentum of 1 a.u. for both electrons to the same side. This acceleration by the laser field drives the electron distribution into the first and third quadrant of figure 4c. Electron repulsion on the contrary tends to drive the electrons to opposite sides and hence into the second and fourth quadrant. Obviously the effect of the driving field

wins over electron repulsion. the observed emission of the electrons to the same side This confirms a recent prediction of Taylor and coworkers [17]. They have solved the time-dependent Schrödinger equation for two electrons in an optical field in three dimensions and found that most of the double ionization probability flux emerges to the same side. Similar conclusions have been drawn from one-dimensional model calculations [18].

One might expect that since, in the single-photon case, no field is active one would observe the opposite and the three-body wave function would evolve purely driven by the electron-electron repulsion. Figures 4a and b and the quicktime movie to figure 4, however, show that the situation is more complicated. In addition to the mutual Coulomb interactions, the field free evolution of the three-body continuum state is governed by the symmetry of the three-body wave function. Since one photon is absorbed by the He ground state, the final state has to have $^1P^o$ symmetry. This results in selection rules leading to several nodes in the three-body momentum distribution (see [19]). The two most important ones are:

1. The two electrons cannot be emitted back to back with equal energy (ungerade parity)
2. If electron 1 is emitted with a polar angle ϑ_1 with respect to the polarization axis, there is a cone shaped node for the second electron at a polar angle $\vartheta_2 = 180 - \vartheta_1$.

While Coulomb repulsion drives the electrons to the opposite direction, the symmetry forbids the energetically most favorable case of back-to-back emission. These symmetry requirements are what makes the distributions in figure 4 a and b so different. If one considers only the direction perpendicular to the polarization, the effect of electron repulsion is most clearly visible. Most of the events are found in the second and fourth quadrant of the figure, which means emission to different half spheres if momentum space is divided by a plane parallel to the polarization. For the momentum component parallel to the polarization, the effect of repulsion is masked by the symmetry requirements as we will show in some more detail in the following.

The emission pattern shown in figure 4 are the result of a projection of a richly structured 6-dimensional space onto a 2-dimensional plane. As the Quicktime Movie of figure 4 shows, the results are strongly dependent on the orientation of this plane of projection. Contrary to the strong field case for single-photon double-ionization this probability distribution in the 6 dimensional space was successfully mapped experimentally. For single photon absorption the quicktime movie figure 5 shows a representative fraction of this distribution in a polar presentation without integration over any coordinate. We have chosen equal energy sharing between the two electrons and plotted the angular distribution of electron 2 for fixed direction of electron 1 (indicated by the arrow) with respect to the polarization axis (which is horizontal). The nodes enforced by the selection rules are shown by the blue and the red dotted line (compare also the rich work on (e,2e) [20]). The figure highlights the influence of the symmetry requirements as the electron flux flows in the region of allowed phase space. In figure 4 the momentum components of the two electrons are shown on the horizontal and vertical axis (parallel to the polarization, left panel, and perpendicular to the polarization, right panel) The angular distributions make obvious that even though both electrons are frequently emitted to the same half sphere, there is always a wide opening angle between them. For the strong field case, presently only the one projection onto the polarization axis as shown in figure 4 (right panel) is available and the full 6 dimensional momentum space has not yet been completely mapped. It can be expected however that the influence of the selection rules on figure 4(right) will be less dramatic for two reasons. First the data are averaged over even and odd numbers of absorbed photons i.e. both parities

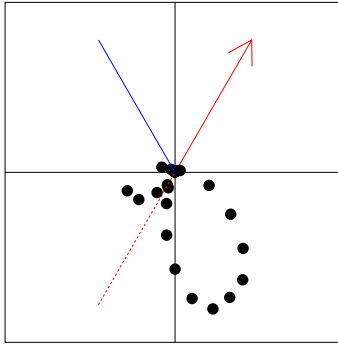


Fig. 5. Double ionization of helium by single photon absorption at 99 eV. The electrons have equal energies. One electron is emitted along the red arrow, the angular distribution of the second electron is shown by the data points in a polar plot. The distance from the origin shows the cross section. The blue line shows the location of the node according to selection rule 2 (see text). The dotted red line shows the node according to selection rule 1 (see text). The polarization axis is horizontal. The Quicktime Movie (1.7MB) shows the change of the distribution as the direction of the first electron changes its angle with respect to the polarization axis

contribute to the final state. Second the angular momentum state of the residual argon ion is not experimentally resolved, again mixing both parities (see [21] for a theoretical study of such angular distributions for the multi-photon case).

5 Conclusions

Double ionization by single photon absorption at low photon energies and multi-photon absorption in the regime of the knee of the double ionization yield are both mediated by an electron-electron scattering mechanism. Shake-off becomes important only for the single photon ionization at higher photon energies (see [22, 23, 24, 25]) and is completely negligible in the multi-photon case ([26, 27]). In both cases this theoretical finding can be confirmed by the experimentally observed momentum distributions of the reaction products. The details of the evolution of the final state momenta as well as parts of the internal structure of momentum space distributions however is different in both cases.

Compared to the single photon case the experiments for multi-photon absorption are still in their infancy. The lesson learned from the single photon case is that it is necessary to fix the final state of the residual ion as well as to know the number of photons (angular momentum) absorbed. Both have a tremendous influence on the momentum space distributions. A detailed quantum mechanical understanding beyond a simple rescattering model will follow from future experiments with high energy resolution on both electrons for a helium target and corresponding theory, which predicts the observable three-body momentum space distribution in the final state.

6 Acknowledgements

We thank Andreas Becker, Farhad Faisal, Robert Moshhammer, Joachim Ullrich and Stefan Keller for many helpful discussions. This work is supported by DFG, BMBF, GSI and DAAD. R.D. acknowledges support by the Heisenberg-Programm of the DFG. T. W. is grateful for financial support of the Graduiertenförderung des Landes Hessen. H.B. and R.D. gratefully acknowledge support from the Alexander v. Humboldt Foundation. We are indebted to Roentdek <http://www.roentdek.com> for providing the position sensitive detectors for this experiment. The Marburg group thanks the DFG for sup-

port through their SFB383 and their Graduiertenkolleg 'Optoelektronik mesoskopischer Halbleiter'. We are grateful to W.W. Rühle for continuous support. This work was also supported by the US Department of Energy, Office of Science Basic Energy Sciences, Geosciences, and Biosciences Division.